Annals of Biomedical Engineering, Vol. 44, No. 9, September 2016 (© *2016*) pp. 2746–2759
DOI: 10.1007/s10439-016-1554-1

Towards the Development of a Mobile Phonopneumogram: Automatic Breath-Phase Classification Using Smartphones

Bersain A. Reyes,[1] Natasa Reljin,[1] Youngsun Kong,[2] Yunyoung Nam,[2] Sangho Ha,[2] and Ki H. Chon[1]

[1]Department of Biomedical Engineering, University of Connecticut, Storrs, CT 06269, USA; and [2]Department of Computer Science and Engineering, Soonchunhyang University, Asan 336-745, Korea

(*Received 13 July 2015; accepted 22 January 2016; published online 3 February 2016*)

Associate Editor Tingrui Pan oversaw the review of this article.

Abstract—Correct labeling of breath phases is useful in the automatic analysis of respiratory sounds, where airflow or volume signals are commonly used as temporal reference. However, such signals are not always available. The development of a smartphone-based respiratory sound analysis system has received increased attention. In this study, we propose an optical approach that takes advantage of a smartphone's camera and provides a chest movement signal useful for classification of the breath phases when simultaneously recording tracheal sounds. Spirometer and smartphone-based signals were acquired from $N = 13$ healthy volunteers breathing at different frequencies, airflow and volume levels. We found that the smartphone-acquired chest movement signal was highly correlated with reference volume ($\rho = 0.960 \pm 0.025$, mean $\pm$ SD). A simple linear regression on the chest signal was used to label the breath phases according to the slope between consecutive onsets. 100% accuracy was found for the classification of the analyzed breath phases. We found that the proposed classification scheme can be used to correctly classify breath phases in more challenging breathing patterns, such as those that include non-breath events like swallowing, talking, and coughing, and alternating or irregular breathing. These results show the feasibility of developing a portable and inexpensive phonopneumogram for the analysis of respiratory sounds based on smartphones.

Keywords—Breath-phase classification, Respiration, Smartphone, Smartphone video camera, Tracheal sounds, Chest movements, Phonopneumogram.

Address correspondence to Ki H. Chon, Department of Biomedical Engineering, University of Connecticut, Storrs, CT 06269, USA. Electronic mail: ki.chon@uconn.edu, kchon@engr.uconn.edu

INTRODUCTION

Computerized Respiratory Sound Analysis (CORSA) has overcome some limitations of the mechanical stethoscope and accelerated the interest in respiratory sound analysis over the last decades.[40] For example, employment of CORSA systems allows quantification of changes in respiratory sound characteristics, correlation of these sounds to other physiological signals, and generation of data representations useful in the diagnosis and treatment of patients with pulmonary diseases.[7] Even with these advantages, pulmonary auscultation with the stethoscope still guides in diagnosis when other tests are not available.[28] Ubiquity, low-cost, mobility, ease-of-use, and non-invasiveness are some characteristics that made the stethoscope the most widely used instrument in clinical practice. Such characteristics should remain when aiming for the development of a CORSA system.

The advanced state-of-the-art of smartphones and their near-ubiquity make them an attractive option for developing a CORSA system that provides more useful information than the stethoscope. Employment of smartphones has advantages over other architectures in terms of implementation and integration with other health monitoring technologies given their hardware and software capabilities. Nowadays, smartphone vital sign applications have been found to be accurate and robust in areas such as cardiac and respiratory monitoring.[17,23]

Automatic classification of breath phases, i.e., automatic labeling of a breath phase as inspiration or expiration, attracts particular interest in applications requiring the timing of breath phases, e.g., when studying the breathing modulation of flow in the heart,[45] or during acoustical airflow[46] and volume estimation[33] to correctly assign the polarity of the estimated signals.

In the field of respiratory sounds, discriminating between inspiratory and expiratory phases is also important when analyzing breathing (base) sounds as well as adventitious sounds. The timing of crackle sounds—short duration (discontinuous) with an explosive character[39]—must be characterized and it has been found to differ between different pulmonary disorders, reflecting different pathophysiology.[30] For example, late inspiratory crackles have been associated with restrictive pulmonary diseases while early inspiratory crackles with severe airway obstruction[24]; early timing of crackles in COPD was found not to overlap with late inspiratory crackles in fibrosing alveolitis.[31] Expiratory crackles can be found in many respiratory diseases,[30] e.g., low-frequency expiratory crackles occur especially in chronic airway obstruction, but in general they are less frequent than inspiratory crackles.[44] Similarly, the relationship of continuous adventitious sounds such as wheezes—long duration sounds with a musical character[39]—to the breath phase is useful for their characterization.[20] The severity of bronchial obstruction has been found to be less in asthmatic patients with only expiratory wheezes than in patients with both inspiratory and expiratory wheezes.[37] Inspiratory short duration wheezes (squawks) are commonly heard in pulmonary fibrosing diseases and pneumonia.[8,27] Regarding base lung sounds, statistically-significant differences were found between healthy and extrinsic allergic alveolitis patients,[5] where the differences were more consistent during the expiratory phase presumably due to the more central source of the expiratory sounds that could carry out more information. Classically, by using phonopneumography—simultaneous presentation of respiratory sound and airflow or volume signals—the timing or volume level of occurrences of adventitious sounds and breath phases can be performed accurately.[30] However, outside clinical and research settings these airflow or volume signals cannot always be taken for granted.

The idea of developing a portable system for respiratory sound analysis is not new,[10,14] nor is the idea of using smartphones for such purposes.[25] Recently, our research group also proposed a smartphone-based system for tracheal sound acquisition purposes.[35] That study was intended to show that smartphones allow acquisition of tracheal sounds that resemble the main characteristics reported in the classical literature,[3,15,19,29,38] such as temporal intensity variation that correlates with airflow, similar frequency content of breath phases at similar airflow peaks, and their use for breath-phase onset detection and respiratory rate estimation. We analyzed the acquired sounds employing a Shannon entropy (SE) estimator together with a joint time–frequency technique in order to obtain time-varying respiration rate estimates, which were found to correlate well when compared to reference values from spirometer-acquired signals.[35] The breath-phase onset estimates based on smartphone-acquired tracheal sounds were found to be around 52 ± 51 ms (mean $\pm$ SD), which are adequate for research involving heart function coupled to respiration.[45] Automatic breath-phase classification was not performed in that pervious study.

Use of tracheal sound measurements for estimating ventilation parameters is of particular interest in the CORSA field, e.g., phonospirometry provides fairly accurate estimates of airflow[46] and tidal volume.[33] Recently, our research group applied a fractal analysis approach for tidal volume estimation from smartphone-acquired tracheal sounds, and it was found that reasonable estimates could be obtained even for measurements 5 days after calibration using a simple bag at a known volume.[34] Besides the promising results in phonospirometry using tracheal sounds, airflow and volume estimators share a necessary step involving the correct classification of the inspiratory and expiratory phases which is usually performed *via* an additional signal, e.g., airflow from a spirometer.

Previous studies using a multichannel CORSA system addressed the classification of breath phases using only respiratory sounds. By employing tracheal sounds for breath-phase onset detection and lung sounds for breath-phase classification, *via* the inspiratory/expiratory power difference, even 100% accuracy was achieved.[21] However, the recording of an additional channel was required in order to achieve this. Hence, this former approach is not feasible in a single channel scenario. Its implementation in a smartphone-based CORSA system would require additional hardware to simultaneously acquire two sound channels if intended for tracheal sound analysis. On the other hand, the use of only tracheal sounds for both breath-phase onset detection and breath-phase classification has also been attempted.[1,2,13,15] By taking advantage of fast changes in tracheal sound intensity, classification has been performed in prior studies using both time and frequency analyses.[13] Unfortunately, the accuracy was not reported in the latter case. More recent studies on this classification task have also reported the use of only tracheal sounds, recorded either over the trachea or close to the nostrils or mouth in agreement with current definitions.[39] By applying a ratio of frequency magnitudes at high and low frequency bands to discriminate between inspiratory and expiratory phases, 97% of 436 phases were correctly classified when compared to respiratory inductance plethysmography.[2] An accuracy of 95.6% was obtained by extracting features from the logarithm of the variance and comparing the current phase to the prior and post phases, with the results being independent of the airflow levels.[15] A 90% accuracy for inhalation and exhalation classification was achieved by applying a threshold level to Mel-frequency cepstral coefficients extracted from tracheal sounds.[1] As was pointed out by other authors, breath-phase detection is a relatively easy task if lung sounds are used; however, as can be noticed from the reported accuracy results, ranging from 90 to 97%, it is still a topic of ongoing research exploration when employing only tracheal sound recordings. Certainly, there are applications when only recording a single respiratory signal is desirable, and classification of breath phases only from tracheal sounds is advantageous; however, more often other physiological signals are simultaneously recorded in order not only to enhance the performance of the monitoring system but also to gain a deeper knowledge of the phenomena under analysis.

This study is intended as a step forward towards the development of a mobile CORSA system that takes advantage of smartphone capabilities. Given that smartphones now have a broad collection of sensors, it is natural to question if the employment of additional smartphone-acquired respiratory signals would be helpful when developing a mobile CORSA system. Therefore, as an alternative to the approach of classifying breath phases using only tracheal sounds we propose to acquire an additional respiratory-related signal that can be used as a temporal reference, as it is done in classic phonopneumography, without the need to plug additional hardware into the smartphone. In particular, we propose using a smartphone-acquired optical signal that tracks chest movements from which the correct detection of the inspiratory and expiratory phases could be achieved by a simple processing technique directly on the smartphone.

Optical approaches have been used for monitoring cardiac and respiratory parameters.[4,32,42] Recently, a breathing pattern tracking algorithm was implemented on a personal computer by detecting shoulder displacements *via* webcam and image processing techniques.[36] In contrast to this study, our research group implemented an application directly on an Android smartphone that recorded chest movements for average respiratory rate estimation.[22] Similar to the study by Shao *et al.*,[36] we noticed that smartphone-based optical signals resemble the spirometry-based volume with the uphill and downhill segments corresponding to the inspiratory and expiratory phases. The proposed smartphone application was previously developed by our research group for non-contact respiratory rate estimation,[22] and this study is an extension to that work which now intends to perform automatic breath-phase classification for respiratory sound analysis. Here, as a reference to compare the classification results, spirometer-based airflow and volume signals were simultaneously collected with the chest movement signal recorded remotely from the smartphone's camera. Tracheal sounds were also simultaneously acquired *via* smartphone as proposed in our previous study[35] during noise-free recordings and also while the subjects made non-breath noise (swallow, cough, and talk) and performed both regular (alternate phases) and irregular breathing patterns to analyze the performance of the proposed classification method in such scenarios.

MATERIALS AND METHODS

Subjects

Thirteen ($N = 13$) healthy and non-smoker volunteers (twelve males), ages ranging from 19 to 52 years (27.77 ± 9.41, mean $\pm$ SD), weights 70.77 ± 8.39 kg, and heights 175.31 ± 6.28 cm, were recruited for this study. Students and staff members from the University of Connecticut (UConn), USA, constituted the group of volunteers. Subjects with previous pneumothorax, with chronic respiratory illnesses such as asthma, and anyone who was currently ill (e.g., common cold or upper respiratory infection) were excluded from participation. The Institutional Review Board of UConn approved the study protocol which was provided to each volunteer for his/her agreement and signature.

Respiration Signals Acquisition

Equipment and Chest Movement Algorithm

Three types of signals were recorded during the breathing maneuvers of each volunteer: airflow and volume signals *via* a spirometer, chest movement signals *via* a smartphone video camera, and tracheal sounds *via* an acoustical sensor plugged into a smartphone audio input. The spirometer system used for recording the respiratory airflow, and corresponding volume *via* integration over time, consisted of a respiration flow head connected to a differential pressure transducer (MLT1000L, FE141 Spirometer, ADInstruments, Inc., Dunedin, New Zealand). A 16-bit A/D converter (PowerLab/4SP, ADInstruments, Inc.) was used to sample the analog airflow and volume signals at 1 kHz. Each volunteer received a new disposable filter, reusable mouthpiece, and disposable nose clip compatible with the spirometer system (MLA304, MLA1026, MLA1008, ADInstruments, Inc.). Prior to each volunteer's experiment, the spirometer system was calibrated using a 3.0 liter calibration syringe

(Hans Rudolph, Inc., KS, USA), following instructions in the manufacturer's manual. The digitized volume signal was regarded as a reference for breath-phase classification.

At the same time that the airflow and volume signals were being recorded, each volunteer's chest movement signal was also recorded, using the frontal camera of an HTC One M8 smartphone (HTC Corporation, Taiwan), which consisted of a 5 MP camera with 1080p full HD video recording at 30 frames-per-second (fps) and wide-angle lens. An algorithm was implemented in the smartphone by our research group using the Java programming language (Oracle Corporation, CA, USA). The implemented algorithm recorded the chest wall motions at a sampling frequency of 25 Hz during the volunteer's maneuvers.[22]

It has been shown that during breathing, as in all mechanical systems involving volume displacement, a relationship between volume displacement and linear motion exists, where the rib cage and abdomen compartments of the chest wall are the major contributors.[16] Chest wall movements in the anteroposterior direction are greater than those in the vertical or transverse directions, with an increase of around 3 cm in the anteroposterior diameter over the vital capacity range.[16] In non-contact optical monitoring of breathing, a video camera captures the changes in the intensity of reflected light caused by these chest wall movements as they modify the path length of the illumination light.[47] Note that in this respiratory monitoring approach, volume changes are not directly measured but a surrogate signal is obtained from analysis of the variations in the reflected light due to chest wall movements captured by the system's camera while breathing. In particular, the algorithm implemented on the smartphone analyzes the average intensities of the red, green and blue (RGB) channels of the video signal within a rectangular region of interest (ROI) at each time instant t as follows:

$$I(t) = \left(\frac{1}{3D}\right) \times \left(\sum_{\{m,n\}\in ROI} i_R(m,n,t) + \sum_{\{m,n\}\in ROI} i_G(m,n,t) + \sum_{\{m,n\}\in ROI} i_B(m,n,t) \right) \quad (1)$$

where D refers to the number of pixels in the ROI, and $i_x(m,n,t)$ refers to the intensity value of the pixel at the m-th row and n-th column of the ROI for the corresponding RGB channel. The ROI was focused on the rib cage area of the subject and consisted of 49×90 pixels selected, i.e., $D = 4410$ pixels, in a resolution of 320×240 pixels. The native resolution and image size of the smartphone's camera is too large for real-time processing and displaying of the data due to the high computational burden. Hence, the Android Camera API (Application Programming Interface) was used to reduce the resolution and size of the ROI. With the settings mentioned above, the frame rate dropped to around 25 fps. In order to obtain the chest movement signal $I(t)$, the video data was first converted in the smartphone from YUV420SP format to RGB using the Open Source Computer Vision library.[26] The implemented app saved the recorded chest movement signal $I(t)$ and time vector of the maneuvers in a text file for further analysis in Matlab (R2012a, The Mathworks, Inc., MA, USA).

A Galaxy S4 smartphone (Samsung Electronics Co., Seoul, South Korea) was employed to acquire tracheal sounds *via* a cabled acoustical sensor composed of a subminiature electret microphone BT-21759-000 (Knowles Electronics, IL, USA) encased in a plastic bell. A double-sided adhesive ring (BIOPAC Systems, CA, USA) was used to affix the acoustical sensor to the volunteers' necks, at the level of the anterior cervical triangle. The Galaxy S4, as well as the HTC One, was running on Android v4.4.2 (KitKat) operating system. The acoustical sensor used in this study was developed by our colleagues at the Metropolitan Autonomous University at Mexico City, and has been successfully used in respiratory sound analysis.[5] The minimum requirements recommended by the European Respiratory Society Task Force Report[7] are satisfied by the Galaxy S4 high-fidelity audio system, and we found that the characteristics and information that can be extracted from this kind of smartphone-acquired sound signal are in agreement with those using regular CORSA systems.[35] After smartphone acquisition of the tracheal sounds at 44.1 kHz and 16-bit per sample, the recorded audio files were transferred to a personal computer for further processing in Matlab.

Maneuver

Each volunteer was asked to breathe through the spirometer system at airflow levels ranging from around 0.5 to 2 L/s, first increasing their volumetric flow rates with each breath for around 1 min, and then decreasing volumetric flow rates with each breath for another minute. These airflow levels cover similar ranges as the ones used in other studies when acquiring tracheal sounds at 'low', 'medium', and 'high' airflows.[15,21,33] Precise minimum and maximum peak airflows varied between volunteers depending on their own manageable levels. For alignment purposes between the different types of recordings, volunteers were asked to perform initial inspiratory and final expiratory apneas of approximately 5 s each and to take a forced respiratory cycle after initial apnea before performing the described maneuver. The airflow signal from the spirometer was displayed on a 40″ monitor placed in front of the volunteers to provide them with visual feedback. During the maneuver, volunteers were in standing still posture and wore nose clips to clamp their nostrils. In order to record the chest movement signal, the smartphone was held in a 3-pronged clamp placed in front of the volunteers at approximately 60 cm from their thorax level so that the central portion of their rib cage areas was captured by the rectangular ROI of 49 × 90 pixels defined in the smartphone application. In a real-world application, the distance from the camera to the subject's thorax would be affected by their body proportions, so it would be necessary to ensure that the ROI's vertical borders do not exceed the anterior axillary line. We have found that a reliable chest movement signal could be obtained even when the ROI captures a smaller area than that defined by the midclavicular lines. Experiments were performed in a regular dry laboratory, not an anechoic chamber, illuminated with ordinary fluorescent ceiling lights. The laboratory was held quiet during each volunteer's maneuvers. Volunteers were asked not to wear loose clothes but they were free to wear any pattern, e.g., plain or stripes, and any color of clothing during the maneuvers. Figure 1 shows an example of the setup during a maneuver acquisition.

Data Preprocessing

Airflow and volume signals from the spirometer were down-sampled to 25 Hz, and then lowpass filtered at 2 Hz with a 4th-order Butterworth filter applied in a forward and backward scheme to produce zero-phase distortion and minimize start and end transients. Due to fluctuations around the sampling frequency encountered during data acquisition, the chest movement signal was interpolated at 25 Hz *via* a cubic spline algorithm to obtain a fixed sampling rate. The same lowpass filter at 2 Hz applied to spirometer signals was applied to the chest movement signal to minimize high frequency components not related to the respiratory maneuver. Acquired tracheal sounds were down-sampled to 6300 Hz. To minimize heart sounds and muscle interference, the down-sampled tracheal sounds were filtered using a 4th-order Butterworth bandpass filter between 100 and 3000 Hz and applied in a forward and backward scheme.

Due to differences in starting times and delays between the spirometer system and the smartphones, alignment of smartphone-acquired signals was performed with respect to spirometry. For the chest movement signal, a segment of 20 s duration was extracted from each recording at the central portion of the maneuver. The cross-correlation sequence between volume and chest movement segments was computed and the sample lag for which the cross-correlation

FIGURE 1. Recording of breathing signals during the maneuver. A smartphone was placed in front of the volunteer at his/her thorax level in order to record the chest movements directly on this device. Tracheal sounds were acquired with an acoustical sensor plugged into the smartphone. Two separate devices were employed to acquire tracheal sounds and chest movement signals in the first stage of the study. Acquisition of both signals was performed with a single smartphone in the second stage. Airflow and volume signals were also acquired *via* a spirometer system and regarded as temporal reference. Actual breath-phases of the maneuver were obtained from volume signal.

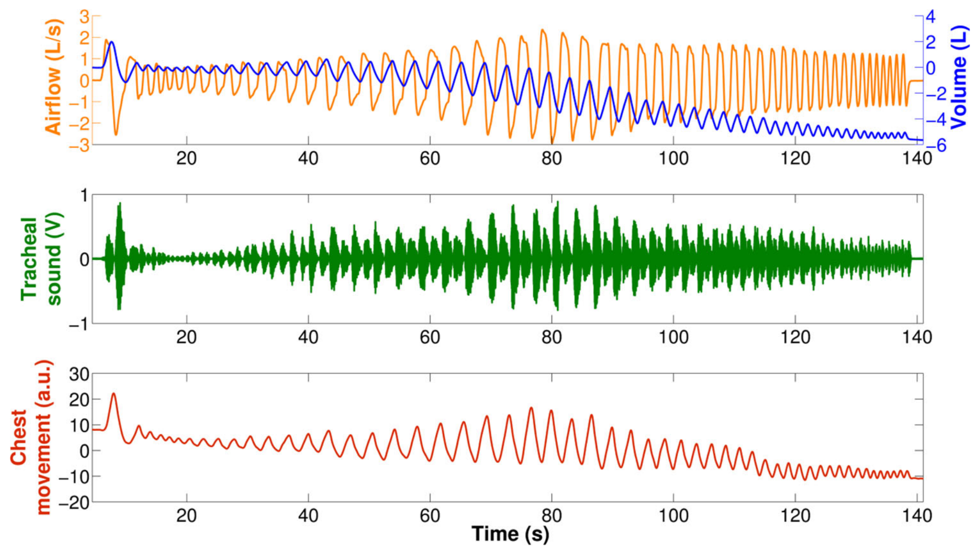

FIGURE 2. Example of acquired signals during the respiration maneuver of a volunteer. Top: spirometer-acquired airflow (orange) and volume (blue) signals. Middle: smartphone-acquired tracheal sounds. Bottom: smartphone-acquired chest movement signal. Observe that despite of the baseline drift and different starting times, the breath-phase onsets are noticeable in both reference volume from spirometer and chest movement signal from smartphone's camera.

value resulted in a maximum was used to shift the smartphone-acquired signal accordingly. For the alignment of tracheal sounds, the SE signal was employed as it resembles a rectified version of the airflow signal,[46] with the breath-phase onsets being indicated by its minima. SE was computed in a moving window scheme *via* the Parzen's density estimation method with a Gaussian kernel[6] using the parameters detailed in our previous study.[35] Then, the tracheal sound was shifted in time so that its initial breath-phase onset after apnea, computed from SE, matched the corresponding onset from the reference volume signal.

Although the manufacturer's instructions were followed, we found a drift in the spirometer-based volume signals. A drift was also found in the smartphone-acquired chest movement signals. Hence, a detrending step based on the empirical mode decomposition (EMD) was applied to both types of signals in order to facilitate their further analysis.[9,12] EMD employs a sifting process that decomposes the original signal in terms of its intrinsic oscillatory modes (IMFs), based only on the original signal, by analyzing the different time scales presented in it. After the sifting process, the original signal $s(t)$ can be represented as

$$s(t) = \sum_{k=1}^{K} IMF_k(t) + r_K(t) \tag{2}$$

where K is the total number of IMFs, and $r_K(t)$ is the residual signal. The EMD sifting process is intended to obtain IMFs without riding waveforms and to produce close to zero mean value as defined by their upper and lower envelope signals.[12] As a result of the sifting process, the first IMFs contain the higher frequency components (lower scales), and hence the trend is contained in the last IMFs. Figure 2 shows an example of raw signals acquired using smartphone and spirometer systems during the breathing maneuver of a volunteer. It is worth mentioning that the initial baseline level in the smartphone-based optical reflectance signal was not set for each patient as it depended on the particular variations of their clothing and illumination background during the recording. Observe that even with the baseline drift found for each subject, the inspiratory/expiratory phases can be noticed as the local increasing/decreasing segments in both the chest movement and reference volume signals. However, signal detrending with EMD, or with a more conventional high-pass digital filter, simplifies further processing including the automatic breath-phase onset detection. An example of the detrended results is shown in Fig. 3.

Breath Phase Classification Using Smartphone Camera Signals

As a reference to test the performance of the proposed breath-phase classification, the spirometer's volume signal was used to obtain the actual breath phases during the maneuver. First, the corresponding breath-phase onsets were found *via* its local maxima and minima. Then, the breath phase between two consecutive onsets was labeled as inspiration or expiration in accordance to the sign of a linear least-squares model[18] fitted on the volume data in that segment (positive: inspiratory phase, negative: expiratory phase).

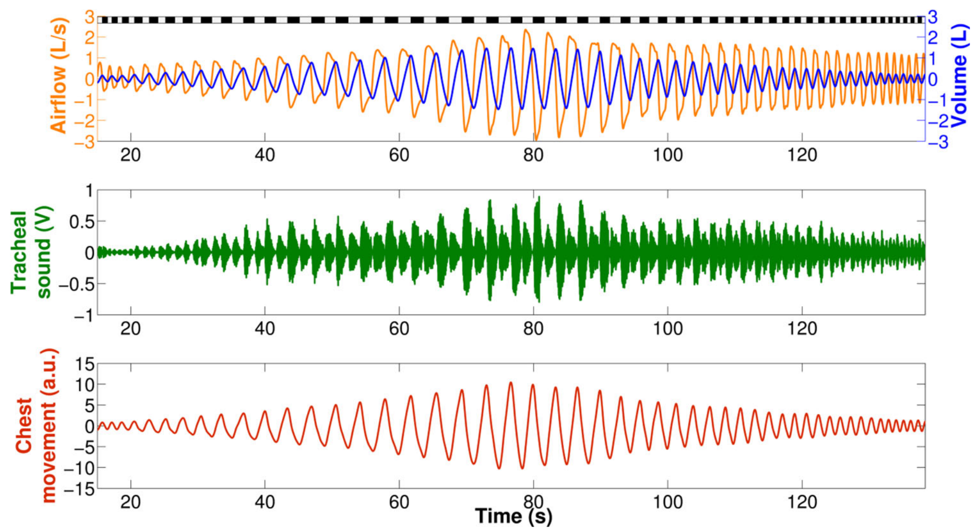

FIGURE 3. Example of preprocessed signals during the breathing maneuver of a volunteer. Top: spirometer-acquired airflow signal (orange) and volume signal (blue) after detrending. Middle: smartphone-acquired tracheal sounds. Bottom: smartphone-acquired chest movement signal with the baseline drift removed after detrend. Gray and black bars displayed on top of spirometer signals indicate the inspiratory and expiratory phases, respectively. Both types of smartphone-acquired signals were aligned in time with respect to reference volume from spirometer.

For the automatic classification of the breath phases using the smartphone-acquired chest movement signal, we propose to take advantage of the linear correlation between the detrended chest movement and the spirometer-based volume signals. As the basis of the proposed method is that the chest movement signal from a smartphone's camera and the spirometer-based volume signal are highly correlated, we quantify this linear correlation during the breathing maneuver by computing the cross-correlation index ρ, defined as:

$$\rho = \frac{\sum_{i=1}^{P} \mathrm{chest}_{\mathrm{smartphone}}(i) \cdot \mathrm{volume}_{\mathrm{spirometer}}(i)}{\sqrt{\sum_{i=1}^{P} \left(\mathrm{chest}_{\mathrm{smartphone}}(i)\right)^2 \cdot \sum_{i=1}^{P} \left(\mathrm{volume}_{\mathrm{spirometer}}(i)\right)^2}} \tag{3}$$

where $\mathrm{chest}_{\mathrm{smartphone}}$ denotes the smartphone-acquired chest movement signal, $\mathrm{volume}_{\mathrm{spirometer}}$ the spirometer-acquired volume signal, and P is the total number of samples of the analyzed signals. If both signals were the same, ρ would equal unity. Hence, values close to 1 indicate high correlation between the signals under analysis. Note that if a high linear correlation between smartphone-acquired chest movement and the reference volume signal is found, it would imply that we could easily obtain accurate breath-phase labels from only the chest movement signal. To this end, the chest movement signal was processed in the same way as the volume signal, i.e., the breath-phase onsets were automatically found in the chest movement signal, then each segment between two consecutive onsets was labeled as inspiration if the sign of the linear least-squares model fitted on the chest movement signal was positive, or as expiration if the corresponding sign was negative, i.e.,

$$\text{Breath phase} = \begin{cases} \text{Inspiration, if } \mathrm{sign}\{\beta\} > 0 \\ \text{Expiration, if } \mathrm{sign}\{\beta\} < 0 \end{cases} \tag{4}$$

where $\mathrm{sign}\{\cdot\}$ refers to the sign function, and β corresponds to the slope of the regression line for the corresponding segment of smartphone data under analysis. For simplicity of notation, let us consider that for every two consecutive breath-phase onsets we have a set of M pairs of smartphone data points denoted by $\{(t_m, y_m)\}_{m=1,\ldots,M}$, where $\{y_m\}_{m=1,\ldots,M}$ refers to the chest movement data from a smartphone, and $\{t_m\}_{m=1,\ldots,M}$ refers to their corresponding time locations at a uniform sampling rate f_s, hence the best linear fit in the least-squares sense has the form $y = \beta t + \alpha$, where the slope β is given by[18]

$$\beta = \frac{\sum_{m=1}^{M} (t_m \cdot y_m) - \frac{1}{M}\left(\sum_{m=1}^{M} t_m\right) \cdot \left(\sum_{m=1}^{M} y_m\right)}{\sum_{m=1}^{M} \left(t_m^2\right) - \frac{1}{M}\left(\sum_{m=1}^{M} t_m\right)^2} \tag{5}$$

Without loss of generality, the relationship between the equidistant time points and the sampling frequency can be used, i.e., $t_m = m \cdot \frac{1}{f_s}$ for $m = 1, \ldots, M$ sample indexes, to rewrite the slope of the linear fit as

$$\beta = \frac{\frac{1}{f_s}\sum_{m=1}^{M} (m \cdot y_m) - \frac{1}{Mf_s}\left(\sum_{m=1}^{M} m\right) \cdot \left(\sum_{m=1}^{M} y_m\right)}{\frac{1}{f_s^2}\sum_{m=1}^{M} m^2 - \frac{1}{Mf_s^2}\left(\sum_{m=1}^{M} m\right)^2} \tag{6}$$

Either Eq. (5) or (6) could be used for breath-phase classification purposes. However, as our interest is only in the sign of the slope it would be more convenient to reduce computational burden when implemented on the smartphone. Using the closed forms of the finite summations given by

$$\sum_{m=1}^{M} m = \frac{M(M+1)}{2}$$
$$\sum_{m=1}^{M} m^2 = \frac{M(M+1)(2M+1)}{6} \quad (7)$$

the Equation of the slope β could be simplified as follows

$$\beta = \left(\frac{6fs}{M(M-1)}\right)\left(\left(\frac{2}{M+1}\right)\sum_{m=1}^{M}(m \cdot y_m) - \sum_{m=1}^{M} y_m\right) \quad (8)$$

In turn, by recognizing that in our case the first term in Eq. (8) is always positive, the sign of the slope β can be easily computed by

$$\text{sign}\{\beta\} = \text{sign}\left\{\frac{2\sum_{m=1}^{M}(m \cdot y_m)}{M+1} - \sum_{m=1}^{M} y_m\right\} \quad (9)$$

Finally, the results of the proposed classification scheme using the smartphone-acquired signal can be expressed in terms of the confusion matrix, where the columns are the actual breath-phases as obtained from spirometry, and the rows are the labeled breath-phases from the chest movement signal from smartphone's camera. The accuracy was obtained from the confusion matrix as

$$\text{Accuracy} = \frac{TP + TN}{P + N} \quad (10)$$

where TP refers to the number of actual inspirations correctly labeled as inspirations, TN to the number of actual expirations correctly labeled as expirations, and P and N to the total number of actual inspirations and expirations, respectively.

RESULTS

Table 1 contains statistics about breath-phase duration, peak airflow, and tidal volume for the breathing maneuvers performed by $N = 13$ volunteers, as measured from spirometer-based airflow and volume signals. The analyzed database was composed of $n_1 = 419$ inspirations and $n_2 = 430$ expirations.

The smartphone-acquired chest movement signal follows the temporal variations of the spirometer-based volume signal during the breathing maneuvers, as shown from the raw data in Fig. 2 and more clearly in Fig. 3 after alignment and detrending. We found a high linear relationship between both detrended signals for all volunteers as measured by the cross-correlation index, $\rho = 0.960 \pm 0.025$. Figure 4 shows an example of the proposed method for automatic breath-phase classification using the smartphone-acquired chest movement signal. Table 2 presents the classification results of the breath phases, as a confusion matrix, for all breathing phases performed by volunteers, where the actual breath phases were obtain from spirometer-acquired volume signals. 100% classification accuracy was achieved as can be seen from the confusion matrix shown in Table 2.

In addition to the previous breathing maneuvers, a couple of volunteers were asked to perform additional breathing patterns according to different scenarios plausible to occur during respiratory recordings, as has been pointed out.[15] Additional recordings included the following scenarios: non-breath noise immersed in regular or irregular breathing, and successive inhalations or exhalations. The scenario with alternating breathing phases with different durations (inspiration–expiration–inspiration–expiration) was not explicitly performed at this time because it was already achieved during the main breathing maneuvers performed by all volunteers. At this stage of the study, the chest movement algorithm was already implemented on the Samsung S4 smartphone so that only this device was employed for both tracheal sounds and chest movements recording. The Samsung S4 frontal camera—2

TABLE 1. Distribution of breath phases' duration, tidal volume, and peak airflow obtained from spirometer during breathing maneuvers (N = 13 subjects. Number of expirations = 430. Number of inspirations = 419).

Parameter	Minimum	Maximum	Mean	Median
Phase duration (s)	0.739 ± 0.317	3.211 ± 1.160	1.749 ± 0.586	1.720 ± 0.670
Inspiration				
Peak airflow (L/s)	0.478 ± 0.176	2.232 ± 1.127	1.107 ± 0.286	1.022 ± 0.263
Tidal volume (L)	0.268 ± 0.131	2.986 ± 0.651	1.292 ± 0.222	1.090 ± 0.215
Expiration				
Peak airflow (L/s)	−0.426 ± 0.203	−2.144 ± 0.875	−1.064 ± 0.361	−0.976 ± 0.346
Tidal volume (L)	−2.972 ± 0.683	−0.236 ± 0.114	−1.261 ± 0.213	−1.062 ± 0.225

Values are presented as mean ± standard deviation.

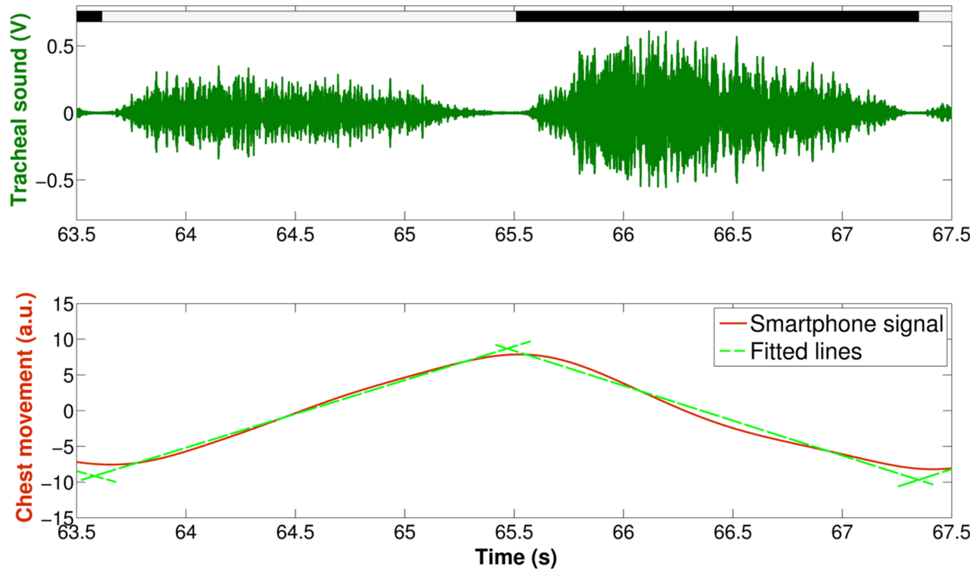

FIGURE 4. Example of automatic breath-phase classification using the smartphone-acquired chest movement signal. Top: smartphone-acquired tracheal sound signal. Gray and black bars displayed on top indicate the inspiratory and expiratory phases, respectively, as measured from reference volume signal from spirometry. Bottom: smartphone-acquired chest movement signal. Superimposed dashed green lines indicate the fitted lines computed *via* least-squares method. Positive and negative slopes of fitted lines were used to label the segment as inspiration and expiration, respectively.

TABLE 2. Breath-phase classification results using smartphone-acquired chest movement signal ($N = 13$ subjects. Number of actual expirations = 430. Number of actual inspirations = 419).

		Actual breath phase (spirometer)	
		Expiration	Inspiration
Classified breath phase (smartphone)	Expiration	430	0
	Inspiration	0	419

MP, 1080p video recording @ 30 fps—was employed for chest movement recording. As before, the native resolution of the Samsung S4 device was not used due to computational burden; its resolution was reduced to 320 × 240 pixels and the ROI was set to 49 × 90 pixels to match those parameters used in the HTC One smartphone. Examples of recorded signals from two volunteers performing different breathing scenarios with non-breathing noises are shown in Figs. 5 and 6. Examples of signals acquired while the volunteers breathed in successive phases are presented in Fig. 7. In Figs. 5, 6 and 7, airflow and volume signals are displayed for temporal reference; gray and black bars displayed on top indicate the inspiratory and expiratory phases, respectively. Fitted lines are superimposed on chest movement signals from the smartphone to show the phase labeling outside the noise event as determined by the corresponding slopes. In Figs. 5 and 6, the noise events are indicated by a red bar. These events were labeled by examining the sound replay and waveform display of the tracheal sounds simultaneously with the chest movement signal from the smartphone, similar to the common practice in respiratory sound analysis, e.g., when labeling adventitious sound events using phonopneumography. Observe that in these cases, the classification of the breath phases is concerned with the phases surrounding the noise events. In Fig. 7, the occurrence of successive inspirations and expirations are also indicated by a red bar, where classification of these breath phases is of concern. By employing the slope of the smartphone signal, these successive phases will be correctly classified with the same phase label given the monotonically increasing (or decreasing) chest movement waveform in such segments.

DISCUSSION

In this paper we propose the automatic classification of inspiratory and expiratory phases from a smartphone-acquired optical recording as an extension to the acquisition of tracheal sounds *via* smartphones. The app we developed allowed real time recording of chest movements during breathing maneuvers directly on the smartphone. For this study, the app was implemented on two Android smartphones, the HTC One M8 and the Samsung Galaxy S4. During the initial stage of the study, recordings of chest movements and tracheal sounds were obtained on two separate smartphones, i.e., the HTC One recorded chest

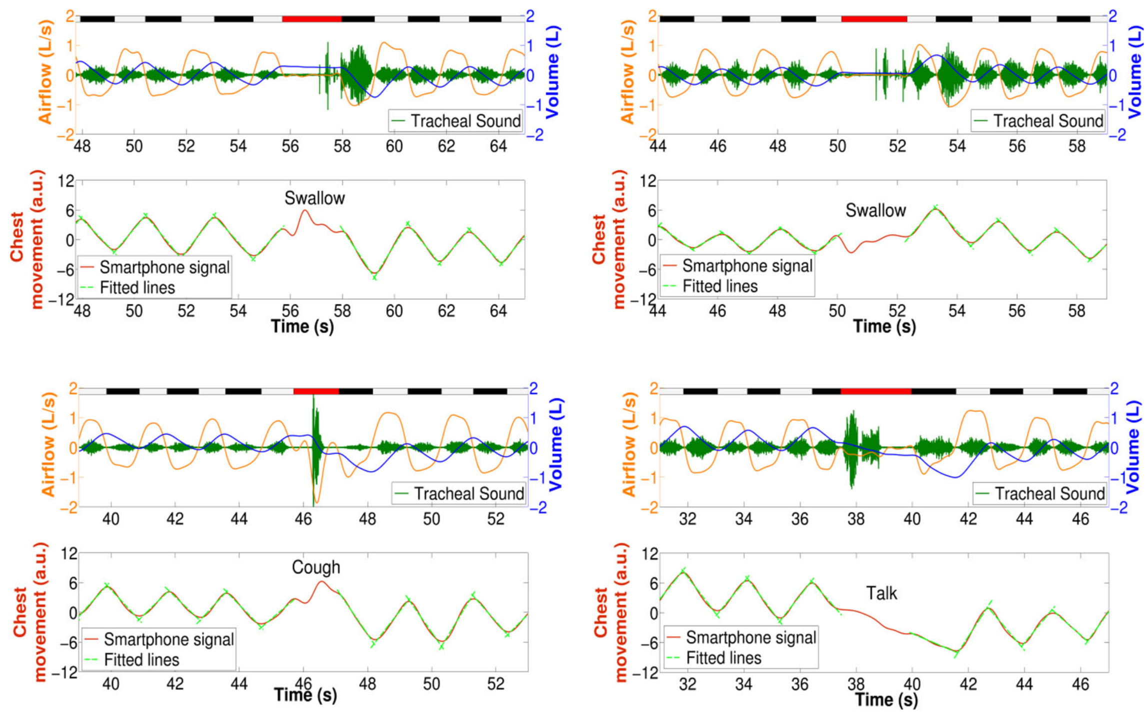

FIGURE 5. Example of smartphone-acquired signals during different scenarios of breathing patterns. For each of the four panels, the upper graph displays the airflow (orange), volume (blue), and tracheal sound (dark green) signals, while the bottom graph displays the chest movement signal (red) and the fitted lines computed *via* least-squares (dashed green lines). Gray/black bars displayed on top indicate the actual inspiratory/expiratory phases measured from spirometry, while the red bar indicates the location of the non-breath noise event. Top left panel: non-breath noise event (swallow) immersed in regular breathing patterns. Top right panel: non-breath noise event (swallow) immersed in irregular breathing. Bottom left panel: non-breath event noise (cough) immersed in regular breathing. Bottom right panel: non-breath noise event (talk) immersed in irregular breathing.

movements and the Galaxy S4 recorded tracheal sounds, as each corresponding smartphone was proposed for that particular use in our previous studies.[22,35] In the second stage of this study, both types of recordings were performed on the same smartphone, i.e., the Galaxy S4 simultaneously recorded chest movements and tracheal sounds.

Previously we studied the employment of smartphones for developing a CORSA system.[35] Results found in that study motivated us to keep working toward the development of a low-cost, easy-to-upgrade, and reliable portable CORSA system. In a subsequent study, our research group aimed for tidal volume estimation using smartphone-acquired tracheal sounds together with novel signal processing techniques and a simple calibration method that does not involve expensive or specialized devices such as spirometers.[34] Although the results are promising, the proposed methods require the correct identification of the inspiratory and expiratory phases.

Phonopneumography has been useful in the field of respiratory sound analysis. When available, it is used as temporal reference for detection and classification of breath phases as well as diverse time events occurring during the breathing maneuver. Accordingly, the correct classification of breath phases proves to be relevant when performing automatic analysis of respiratory sounds containing adventitious sounds,[20,30] as well as for applications involving airflow or volume estimation from tracheal sounds.[33,45,46] Given the promising estimation of ventilation parameters, the use of only tracheal sounds has been proposed to address the automatic classification of breath phases.[1,2,13,15] Although this approach has advantages, e.g., greater user acceptance of the acoustical sensors in comparison to nasal cannulas or facemasks used to measure airflow, its accuracy results for breath-phase classification have not matched those found when using an additional lung sound channel.

Given the importance of the correct breath-phase classification in the CORSA field, and as a more-accurate alternative to using only tracheal sounds, we studied the employment of an additional respiration-related signal that could easily upgrade a mobile smartphone-based system. In this paper, instead of attempting the classification of breath phases from tracheal sounds, we employed an optical approach to perform this task. Previously, our research group implemented an algorithm that allows the estimation of average respiratory rate from a smartphone-ac-

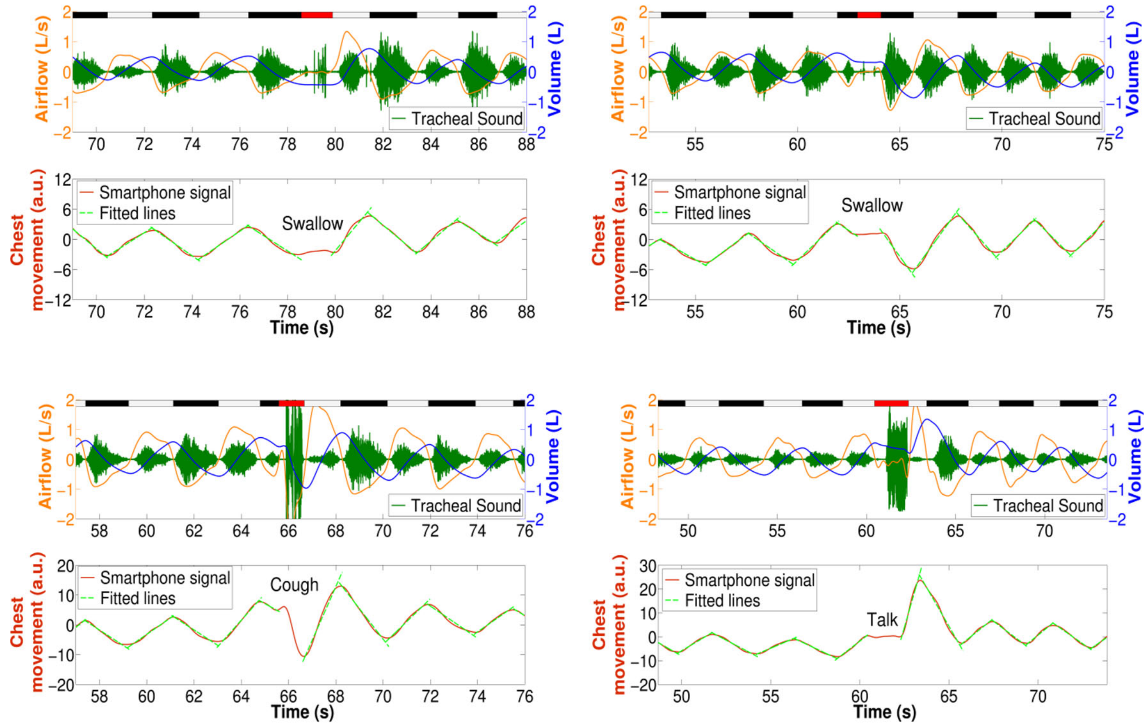

FIGURE 6. Example of smartphone-acquired signals during different scenarios of breathing patterns of a second volunteer. For each of the four panels, the upper graph displays the airflow (orange), volume (blue), and tracheal sound (dark green) signals, while the bottom graph displays the chest movement signal (red) and the fitted lines computed *via* least-squares (dashed green lines). Gray/black bars displayed on top indicate the actual inspiratory/expiratory phases measured from spirometry, while the red bar indicates the location of the non-breath noise event. Top left panel: non-breath noise event (swallow) immersed in regular breathing patterns. Top right panel: non-breath noise event (swallow) immersed in irregular breathing. Bottom left panel: non-breath noise event (cough) immersed in regular breathing. Bottom right panel: non-breath noise event (talk) immersed in irregular breathing.

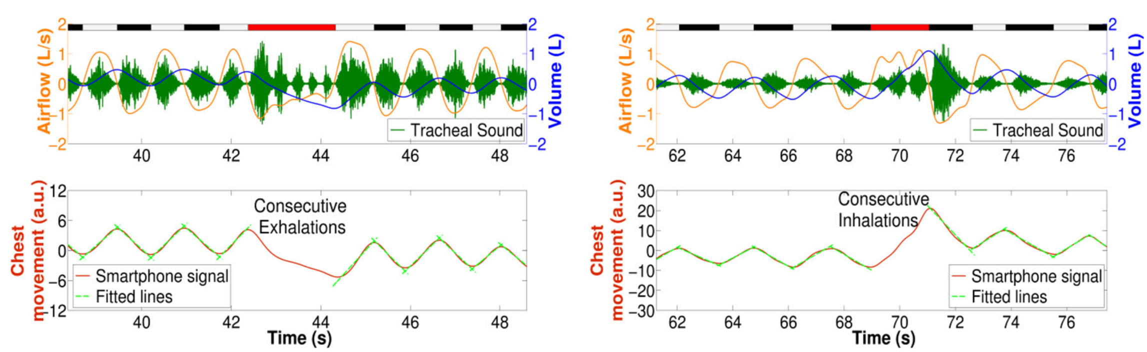

FIGURE 7. Example of acquired respiratory signals while a couple of volunteers were taking successive breaths. For each of the two panels, the upper graph displays the airflow (orange), volume (blue), and tracheal sound (dark green) signals, while the bottom graph displays the chest movement signal (red) and the fitted lines computed *via* least-squares (dashed green lines). Gray/black bars displayed on top indicate the actual inspiratory/expiratory phases measured from spirometry, while the red bar indicates the location of the successive breaths event. Left panel: consecutive exhalations. Right panel: consecutive inhalations.

quired chest movement signal,[22] and we noticed that this signal resembles the spirometer-acquired volume signal. To investigate our previous visual observations, in this study were compared the spirometer-based volume and the smartphone-based chest movement signal using the cross-correlation index. The chest movements and tracheal sounds were recorded on separate smartphones at the initial stage of the study because the optical algorithm had been only implemented on a different smartphone from the one used to record tracheal sounds in our previous studies. We found that both types of signals were highly correlated ($\rho = 0.960 \pm 0.025$, mean $\pm$ SD), corroborating our initial observations. These results indicate that our smartphone-based monitor is able to capture the intensity changes in the reflected light caused by the chest motion, linearly related to volume, while breathing. According to Konno and Mead,[16] this motion-volume linear relationship is attributable to the relative smaller diameter changes while breathing in comparison to the absolute diameter of the chest wall, and to the larger contribution of the anteroposterior diameter changes compared to the vertical or transversal. This linearity appears to hold in the recorded optical chest movement signal from a smartphone's camera. Hence, the volume signal was employed to label the phases of the respiratory maneuvers, while the chest movement signal was processed using a simple linear regression to label the uphill segments as inspirations and downhill segments as expirations based on the slope of the computed model. We found 100% accuracy for the task of breath-phase classification, i.e., all inspiratory phases ($n_1 = 419$) were detected as inspirations and all expiratory phases ($n_2 = 430$) were detected as expirations, for the maneuvers performed by the volunteers in standing still posture, while breathing at different cycle durations ranging from 700 ms to 3 s, and different airflow levels with peaks ranging from 0.5 to 2.0 L/s.

The second stage of the study was intended to analyze the performance of the chest movement signal for the automatic classification of breath phases during different scenarios of breathing patterns that included non-alternate inspiratory and expiratory phases, as well as non-breathing related noises like swallowing, talking and coughing. At this point, the optical algorithm was already implemented on the same smartphone tested for tracheal sound acquisition, so that in this stage only a single smartphone was employed. As stated by other authors, these different breathing patterns are the most challenging in respiratory phase detection.[15] We found that the proposed classification scheme can be used to correctly classify the breath phases in such scenarios. For the non-breath events immersed in typical alternate breathing (e.g., inspiration-noise-expiration) or in irregular breathing (e.g., expiration-noise-expiration), the algorithm was able to classify the breath phases surrounding these noise events as indicated by the corresponding slopes of the chest movement signal from the smartphone. During the scenarios involving consecutive inspirations or consecutive expirations, the tracheal sounds involved were correctly classified as the same phase given the fitted slope for the chest movement signal in that time interval.

Besides the above-mentioned results, we recognize limitations of this study. First, subjects were instructed to stand still while performing the breathing maneuvers, and hence, the performance deterioration due to body motion artifacts, not related to the breathing maneuver, was not explored. Incorporation of body tracking and artifact removal algorithms similar to those proposed in the literature to reduce such motion effects—for example in[36,41]—is a topic of further exploration towards the development of our mobile system. Second, we only explored recordings with the subjects in standing posture. Recordings in supine posture were not performed. We foresee that the proposed scheme would bring similar classification results to the ones reported here when the visual field of the smartphone's camera is focused on the area with the most dominant contribution to volume while breathing, e.g., the abdominal compartment in supine posture.[16] Third, recordings were performed in a regular indoor laboratory, and hence further experiments are required to analyze the usability of the proposed portable system in different outdoor environments to fully take advantage of its mobility.

This study represents a step forward in the development of a mobile system for the analysis of respiratory sounds that takes advantage of additional sensors already existing in smartphones. The obtained results show that simultaneous recordings of tracheal sounds and chest movements are useful for both automatic classification of the breath phases and correct timing of events such as the ones shown in this paper. An interesting alternative to our proposed approach and a topic for future exploration involves the use of accelerometers for respiratory sound recording[11,43] with the potential benefit that information regarding the breath phase could be extracted, especially for lung sound recordings, in addition to the respiratory sound itself. Currently, motivated by the high linear correlation obtained between the chest movement signal from the smartphone's camera and the reference volume from spirometry, we are working on a study involving the feasibility of estimating tidal volume *via* the smartphone-acquired chest movement signal so that estimation of this parameter could be easily performed outside research and clinical settings. Finally, we consider that the smartphone approach proposed in this study, as well as similar ones for respiratory monitoring, has the potential to be readily accepted by users due to its simplicity and comfort as well as potential to reach populations and geographic areas where it is difficult to study respiratory sounds with current computerized methods.

ACKNOWLEDGMENTS

This work is supported in part by the US Army Medical Research and Material Command (USAMRMC) under grant No. W81XWH-12-1-0541.

The authors would like to thank Professors Sonia Charleston-Villalobos, Tomas Aljama-Corrales, and Ramon Gonzalez-Camarena for introducing an acoustical sensor used in this study.

REFERENCES

[1]Abushakra, A., and M. Faezipour. Acoustic signal classification of breathing movements to virtually aid breath regulation. *IEEE J. Biomed. Health Inform.* 17:493–500, 2013.

[2]Alshaer, H., G. R. Fernie, and T. D. Bradley. Monitoring of breathing phases using a bioacoustic method in healthy awake subjects. *J. Clin. Monit. Comput.* 25:285–294, 2011.

[3]Beck, R., G. Rosenhouse, M. Mahagnah, R. M. Chow, D. W. Cugell, and N. Gavriely. measurements and theory of normal tracheal breath sounds. *Ann. Biomed. Eng.* 33:1344–1351, 2005.

[4]Cala, S. J., C. M. Kenyon, G. Ferrigno, P. Carnevali, A. Aliverti, A. Pedotti, P. T. Macklem, and D. F. Rochester. Chest wall and lung volume estimation by optical reflectance motion analysis. *J. Appl. Physiol.* 81:2680–2689, 1996.

[5]Charleston-Villalobos, S., L. Albuerne-Sanchez, R. Gonzalez-Camarena, M. Mejia-Avila, G. Carrillo-Rodriguez, and T. Aljama-Corrales. Linear and nonlinear analysis of base lung sound in extrinsic allergic alveolitis patients in comparison to healthy subjects. *Methods Inf. Med.* 52:266–276, 2013.

[6]Duda, R. O., P. E. Hart, and D. G. Stork. Pattern classification. New York: Wiley, p. 679, 2000.

[7]Earis, J. E., and B. M. G. Cheetham. Current methods used for computerized respiratory sound analysis. *Eur. Respir. Rev.* 10:586–590, 2000.

[8]Earis, J. E., K. Marsh, M. G. Pearson, and C. M. Ogilvie. The inspiratory ‘‘squawk’’ in extrinsic allergic alveolitis and other pulmonary fibroses. *Thorax* 37:923–926, 1982.

[9]Flandrin, P., P. Goncalves, and G. Rilling. Detrending and denoising with empirical mode decomposition. In: Proceedings of the 12th European Signal Processing Conference (EUSIPCO'04), pp. 1581–1584, 2004.

[10]Guangbin, L., C. Shaoqin, Z. Jingming, C. Jinzhi, and W. Shengju. The development of a portable breath sounds analysis system. In: Proceedings of the 14th Annual International Conference of the IEEE Engineering in Medicine and Biology Society, pp. 2582–2583, 1992.

[11]Hu, Y., E. G. Kim, G. Cao, S. Liu, and Y. Xu. Physiological acoustic sensing based on accelerometers: a survey for mobile healthcare. *Ann. Biomed. Eng.* 42:2264–2277, 2014.

[12]Huang, N. E., Z. Shen, S. R. Long, M. C. Wu, H. H. Shih, Q. Zheng, N.-C. Yen, C. C. Tung, and H. H. Liu. The empirical mode decomposition and the Hilbert spectrum for nonlinear and non-stationary time series analysis. *Proc. R. Soc. Lond. Ser. Math. Phys. Eng. Sci.* 454:903–995, 1998.

[13]Hult, P., B. Wranne, and P. Ask. A bioacoustic method for timing of the different phases of the breathing cycle and monitoring of breathing frequency. *Med. Eng. Phys.* 22:425–433, 2000.

[14]Hung, K., B. L. Luk, W. H. Choy, B. Tai, and S. K. Tso. Multifunction stethoscope for telemedicine. In: Proceedings of the 2003 IEEE International Workshop on Computer Architectures for Machine Perception, pp. 87–89, 2004.

[15]Huq, S., and Z. Moussavi. Acoustic breath-phase detection using tracheal breath sounds. *Med. Biol. Eng. Comput.* 50:297–308, 2012.

[16]Konno, K., and J. Mead. Measurement of the separate volume changes of rib cage and abdomen during breathing. *J. Appl. Physiol.* 22:407–422, 1967.

[17]Lee, J., B. A. Reyes, D. D. McManus, O. Mathias, and K. H. Chon. Atrial fibrillation detection using an iPhone 4S. *IEEE Trans. Biomed. Eng.* 60:203–206, 2013.

[18]Lindfield, G., and J. Penny. Numerical Methods: Using MATLAB. New York: Academic Press, p. 553, 2012.

[19]McKusick, V. A., J. T. Jenkins, and G. N. Webb. The acoustic basis of the chest examination; studies by means of sound spectrography. *Am. Rev. Tuberc.* 72:12–34, 1955.

[20]Meslier, N., G. Charbonneau, and J. L. Racineux. Wheezes. *Eur. Respir. J.* 8:1942–1948, 1995.

[21]Moussavi, Z. K., M. T. Leopando, H. Pasterkamp, and D. G. Rempel. Computerised acoustical respiratory phase detection without airflow measurement. *Med. Biol. Eng. Comput.* 38:198–203, 2000.

[22]Nam, Y., Y. Kong, B. Reyes, N. Reljin, and K. H. Chon. Monitoring of heart and respiratory rates using dual cameras on a smartphone. *PLoS ONE*. In revision, 2016.

[23]Nam, Y., J. Lee, and K. H. Chon. Respiratory rate estimation from the built-in cameras of smartphones and tablets. *Ann. Biomed. Eng.* 42:885–898, 2013.

[24]Nath, A. R., and L. H. Capel. Inspiratory crackles—early and late. *Thorax* 29:223–227, 1974.

[25]Oletic, D., B. Arsenali, and V. Bilas. Towards continuous wheeze detection body sensor node as a core of asthma monitoring system. In: Wireless Mobile Communication and Healthcare, edited by K. S. Nikita, J. C. Lin, D. I. Fotiadis, and M.-T. A. Waldmeyer. Berlin : Springer, 2012, pp. 165–172.

[26]Open CV. Open Source Computer Vision Library at < http://sourceforge.net/projects/opencvlibrary/ >.

[27]Paciej, R., A. Vyshedskiy, D. Bana, and R. Murphy. Squawks in pneumonia. *Thorax* 59:177–178, 2004.

[28]Pasterkamp, H., C. Carson, D. Daien, and Y. Oh. Digital respirosonography. New images of lung sounds. *Chest* 96:1405–1412, 1989.

[29]Pasterkamp, H., S. S. Kraman, and G. R. Wodicka. Respiratory sounds: advances beyond the stethoscope. *Am. J. Respir. Crit. Care Med.* 156:974–987, 1997.

[30]Piirila, P., and A. R. Sovijarvi. Crackles: recording, analysis and clinical significance. *Eur. Respir. J.* 8:2139–2148, 1995.

[31]Piirilä, P., A. R. Sovijärvi, T. Kaisla, H. M. Rajala, and T. Katila. Crackles in patients with fibrosing alveolitis, bronchiectasis, COPD, and heart failure. *Chest* 99:1076–1083, 1991.

[32]Poh, M.-Z., D. J. McDuff, and R. W. Picard. Advancements in noncontact, multiparameter physiological measurements using a webcam. *IEEE Trans. Biomed. Eng.* 58:7–11, 2011.

[33]Que, C.-L., C. Kolmaga, L.-G. Durand, S. M. Kelly, and P. T. Macklem. Phonospirometry for noninvasive measurement of ventilation: methodology and preliminary results. *J. Appl. Physiol. Bethesda Md* 1985(93):1515–1526, 2002.

[34]Reljin, N., B. A. Reyes, and K. H. Chon. Tidal volume estimation using the blanket fractal dimension of the tracheal sounds acquired by smartphone. *Sensors* 15:9773–9790, 2015.
[35]Reyes, B. A., N. Reljin, and K. H. Chon. Tracheal sounds acquisition using smartphones. *Sensors* 14:13830–13850, 2014.
[36]Shao, D., Y. Yang, C. Liu, F. Tsow, H. Yu, and N. Tao. Noncontact monitoring breathing pattern, exhalation flow rate and pulse transit time. *IEEE Trans. Biomed. Eng.* 61:2760–2767, 2014.
[37]Shim, C. S., and M. H. Williams. Relationship of wheezing to the severity of obstruction in asthma. *Arch. Intern. Med.* 143:890–892, 1983.
[38]Sierra, G., V. Telfort, B. Popov, M. Pelletier, P. Despault, R. Agarwal, and V. Lanzo. Comparison of respiratory rate estimation based on tracheal sounds versus a capnograph. In: Proceedings of the 27th Annual International Conference of the IEEE Engineering in Medicine and Biology Society, pp. 6145–6148, 2005.
[39]Sovijarvi, A. R. A., F. Dalmasso, J. Vanderschoot, L. P. Malmberg, G. Righini, and S. A. T. Stoneman. Definition of terms for applications of respiratory sounds. *Eur. Respir. Rev.* 10:597–610, 2000.
[40]Sovijarvi, A. R. A., J. Vanderschoot, and J. E. Earis. Standardization of computerized respiratory sound analysis. *Eur. Respir. Rev.* 10:585–585, 2000.
[41]Sun, Y., S. Hu, V. Azorin-Peris, S. Greenwald, J. Chambers, and Y. Zhu. Motion-compensated noncontact imaging photoplethysmography to monitor cardiorespiratory status during exercise. *J. Biomed. Opt.* 16:077010–077010, 2011.
[42]Tarassenko, L., M. Villarroel, A. Guazzi, J. Jorge, D. A. Clifton, and C. Pugh. Non-contact video-based vital sign monitoring using ambient light and auto-regressive models. *Physiol. Meas.* 35:807, 2014.
[43]Vannuccini, L., J. E. Earis, P. Helisto, B. M. G. Cheetham, M. Rossi, A. R. A. Sovijarvi, and J. Vanderschoot. Capturing and preprocessing of respiratory sounds. *Eur. Respir. Rev.* 10:616–620, 2000.
[44]Vyshedskiy, A., R. M. Alhashem, R. Paciej, M. Ebril, I. Rudman, J. J. Fredberg, and R. Murphy. Mechanism of inspiratory and expiratory crackles. *Chest* 135:156–164, 2009.
[45]Xiong, C., B. Hök, T. Strömberg, D. Loyd, B. Wranne, and P. Ask. A bioacoustic method for timing of respiration at cardiac investigations. *Clin. Physiol.* 15:151–157, 1995.
[46]Yadollahi, A., and Z. M. K. Moussavi. Acoustical respiratory flow. *IEEE Eng. Med. Biol. Mag.* 26:56–61, 2007.
[47]Zhao, F., M. Li, Y. Qian, and J. Z. Tsien. Remote measurements of heart and respiration rates for telemedicine. *PLoS One* 8:e71384, 2013.